ISBN: 978-3-95450-193-9 doi:10.18429/JACoW-ICALEPCS2017-THPHA154

EXPERIMENT CONTROL WITH EPICS7 AND SYMMETRIC MULTIPROCESSING ON RTEMS

H. Junkes *, H.-J. Freund, L. Gura, M. Heyde, P. Marschalik, Z. Yang
Fritz-Haber-Institute of the Max-Planck-Society, Berlin, Germany

Abstract

We are in the process of setting up a high-speed scanning tunneling microscope (STM) to study the dynamics of the crystal-glass transition. While so far Experimental Physics and Industrial Control System (EPICS)v3 [1] had been sufficient for our conventional experimental STM studies, a new project to study dynamics needs considerably higher data throughput than possible using EPICSv3. For this reason, we control the high-speed-STM with the new EPICS7, using the protocol pvAccess. The development version 3.16 of EPICSv3 and bundleCPP of the EPICSv4-suite are in use. Both of them will be the base components of the new EPICS7 framework. We expect a data rate of 4 Gbit/s for up to 5 hours in order to address dynamic processes in oxide networks structures in real space over a wide range of temperatures.

SCIENTIFIC MOTIVATION

In this project we focus on crystalline and vitreous silica films and their interconversion. Silica is the prototype glass network former and the basis of many glasses. As it is one of the most abundant materials on earth, it is relevant in various branches of modern technologies. While the atomic structure of crystalline materials in general is well understood due to the application of diffraction techniques, the structure of amorphous or vitreous materials such as silica glass is still an open field in research [2]. In fact, diffraction techniques have only been able to deliver pair correlation functions, which reveal the density of a material around a given atom, but do not allow a detailed reconstruction of the atomic structure as in the case of crystalline materials. For the first time, a real space image of a silica glass with atomic resolution was recorded with scanning probe microscopy (SPM) techniques applied to a thin silica film grown atomically flat on a metal substrate [3]. This film has verified the early predictions from 1932 by Zachariasen [4]. Density Functional Theory (DFT) calculations have been performed to look into the energetical differences between crystalline and the simplest model of a vitreous film by exchanging four 6-membered rings into two 5- and two 7-membered rings. The spatial transition from the crystalline to the vitreous phase has already been studied in our group [5]. Under the impact of a probing electron beam structural changes in the the silica film have been observed during transmission electron microscope (TEM) measurements [6]. By monitoring the temperature induced phase transition in real space, we want to shed some light on the dynamics in glasses - especially on the processes occurring during the conversion via a liquid phase during the glass-crystal transition. For this purpose, an SPM is developed that allows the study of the atomic structure over a wide range of temperatures including the two extremes: cryogenic temperatures and the dewetting temperature of the silica film [7]. This instrument may also be used to address a number of other scientific problems in the field of surface science. The achievable scan rate with our SPM seems to be the most critical point in this project.

* junkes@fhi-berlin.mpg.de

TIME RESOLUTION

Inspired by pump-probe techniques [8], time resolution ranging from nanoseconds to subpicoseconds has been achieved in STM experiments by incorporating voltage [9], laser [10] or terahertz pulses [11, 12] into the tunneling junction. Such experiments have allowed to study the dynamics of spins, charge carriers and quasiparticles upon excitation in nanostructures. However, these concepts do not allow for imaging in real space at such time scales.

In order to directly resolve dynamic processes of atom diffusion [13, 14], film growth [15, 16] and chemical reaction [17, 18], a lot of effort has been made to construct an STM that can scan following such processes at time scales ranging from a few seconds down to milliseconds [19, 20].
Here, one bottleneck for fast scanning is the bandwidth of the mechanical loop of the scanner unit. In order to minimize the noise originating from the piezo movement, it is crucial to use piezo elements with a resonance frequency higher than the waveform frequency driving the fast scan of the piezo. Another challenge is the high speed electronics for hardware controlling and data acquisition. Feedback electronics with a bandwidth of 1 MHz and preamplifier with a bandwidth of 600 kHz were developed by Frenken et al. [19], which allow frame rates up to 200 images/s with 256×32 pixels per image scanning with hybrid mode between the constant-height and constant-current modes. Our aim is to build an STM with comparable or even higher frame rates. For this purpose, we designed a hybrid scanner including a large scanner and a small scanner as the STM head (Fig. 1). Both of them are made from segmented tube piezos. The large scanner is controlled by the Nanonis SPM Control System from Specs GmbH [21] and used for large area and slow scan in constant current mode. After a good place is observed in the slow scan, we can start the fast scan in a small area by using the small scanner. The small scanner has a resonance frequency above 1 MHz and is controlled by the FHI High Speed Controller. The fast scan is performed in constant height mode and the tunneling current is measured by a preamplifier with a bandwidth up to 200 MHz from FEMTO Messtechnik GmbH [22], so that no feedback loop is needed

ISBN: 978-3-95450-193-9 doi:10.18429/JACoW-ICALEPCS2017-THPHA154

and the frame rate is mainly limited by the shot noise in the tunneling current measurement [20]. In addition to the high scan speed, being able to heat the sample to high temperature during scanning is necessary to active the phase transition from crystalline to vitreous [7]. Here, the STM head is designed to have an overall cylindrical shape to minimize the thermal drift during heating. Moreover, the microscope is located in a continuous-flow cryostat to keep the piezos below its Curie temperature while the sample can be heated to the desired temperatures.

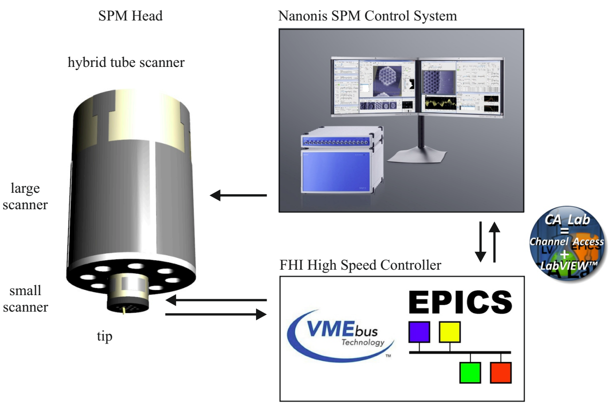

Figure 1: Schematic of the scanner unit combined with two SPM control systems.

CONTROL SYSTEM

EPICS is the software backbone for most of our complex experiments. It comprises a set of tools, network protocols and hardware drivers centered around a highly flexible distributed database of process variables [1]. Even for this project we use EPICS to control the standard (moderate data rate) devices needed to run such an experiment. This includes lock-in amplifiers, oscilloscopes, Versa Module Eurocard-bus (VMEbus) shelf manager, different vacuum equipment (vacuum gauges, turbo and ion pumps), for the sample surface preparation devices such as e-beam-heater, sputter-gun, evaporators, and mass spectrometer with the potential for further additions. Some of these devices were connected to dedicated MOXA terminal [23] servers with RS485 or RS232 conversion interfaces others were connected to a linux based EPICS Input Output Controller (IOC) via a foundry network switch. To communicate with these we are using the well defined EPICS modules ASYN and StreamDevices [24, 25]. The communication for control with the slow-scan vendor lock-in microscope Nanonis from SPECS [21], is realized by using the CA Lab [26] software. Nanonis provides a LabVIEW [27] programming environment for its SPM Control System. This interface allows to programmatically control all Nanonis modules and allows the user to add customized Virtual Instruments (VI). Any VI can use caLabGet.vi to read or caLabPut.vi to write EPICS variables. The Nanonis SPM control system controls the large scanner as shown in Fig. 1. To address the transition from a crystalline to a vitreous phase in real space we had to setup our own control system to run the small scanner unit. Since we have very good long-term experiences with our VMEbus systems, we had selected them for this project too.

VMEbus system - the computer control system for the fast scanner unit consists of:

- Wiener Mini Crate 395 with a CML00.Shelf Manager,
- MVME6100, single board computer for control,
- MVME2500, single board computer for communication,
- HIGHLAND V375, 4-channel arbitrary waveform generator,
- Struck SIS3316, 250 MSPS 14bit digitizer.

Out of the box STM systems scan the sample by applying two triangular signals to the piezos (see Fig. 2).

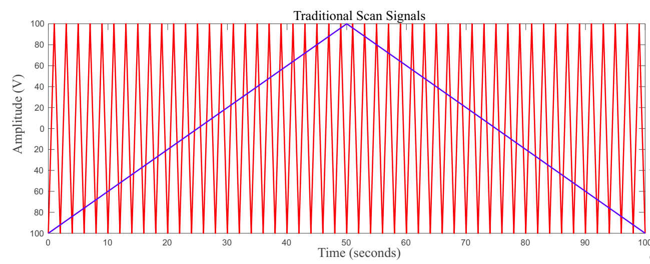

Figure 2: Visualization of the x- (red) and y-signals (blue) for typical STM scanner motion.

In Fig. 3 an atomically resolved vitreous silica film is shown probed with an SPM at low temperature and in ultra high vacuum (UHV). The recording of the 5 x 5 nm^2 image takes more than 10 min with a traditional scan mode. The image shown in Fig. 3 a) is used later on as an input structure for image simulation.

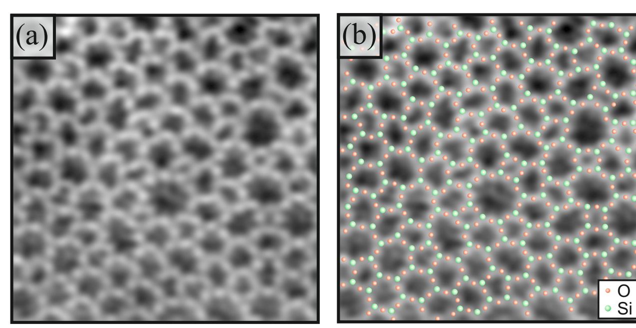

Figure 3: Atomically resolved SPM images of the vitreous silica film. a) shows the atomically resolved contrast obtained with a triangular scan. b) this image has been overlayed with marked positions of the topmost Si (green balls) and O atoms (red balls). Reproduced with permission from [28].

Since at high speeds the reverse movements leads to distortion, this scanning method is not suitable for higher scan rates. In order to achieve higher frame rates we use the capabilities of the waveform generator shown in Fig. 5 [29].

ISBN: 978-3-95450-193-9 doi:10.18429/JACoW-ICALEPCS2017-THPHA154

It enables a smooth variation of the output frequency and amplitude in real time (see Fig. 4) [30].

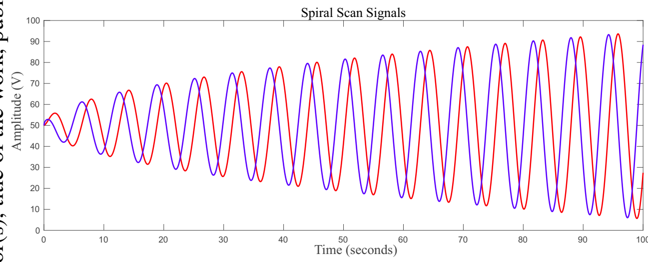

Figure 4: Plotted signals for the spiral scan.

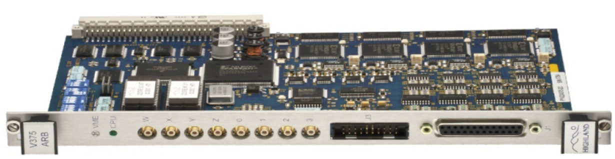

Figure 5: Waveform generator Highland V375 [29].

The waveform generator Highland V375 has the following specifications:

- 4 independent direct digital synthesizer (DDS) frequency sources allow smooth variation of waveform scan rates,
- 4 versatile, memory-table-driven waveform generators scan up to 65,536 discrete points per waveform at up to 15 MHz point step rate,
- 16-bit amplitude and 32-bit frequency resolution,
- Output frequency, amplitude, phase, and DC offset are smoothly variable in real time,
- Versatile wave memory partitioning allows waveform read/write operations concurrent with wave generation, so multiple waveforms can be loaded and selected in real time.

In order to generate the wanted constant linear velocity (CLV) spirals the radius and angular velocity need to be varied simultaneously in a way that the linear velocity of small scanner is kept constant at all times. This can be achieved by varying the frequency of the sinusoidal set points. By varying the amplitude of the sinusoidal set points a spiral trajectory is being traced. A property of this spiral is that its pitch P, which is the distance between two consecutive intersections of the spiral curve with any line passing through the origin, is constant [30].

The equation that generates the spiral with a constant linear velocity v can be derived from the differential equation

$$\frac{\mathrm{d}r}{\mathrm{d}t} = \frac{Pv}{2\pi r} \tag{1}$$

as shown in [30]. Here r and t denote the radius and time, respectively. The pitch is the constant distance between two neighbouring intersections of x-axis and spiral and can be calculated as

$$P = \frac{2R}{n-1} \tag{2}$$

([30], eq. (4)), where R denotes the total spiral radius and n the number of times the spiral curve intersects the x-axis. By varying the sampling frequency of the used struck digitizer (up to 250 MSPS) [31] we can control the number of points we want to acquire. In order to achieve the highest possible image refresh rate, we apply mathematical interpolation to the image data to minimize the number of pixels required (see Fig. 6).

Given the data points at some spiral points it is necessary to interpolate these values on a regular grid. For this the scipy.interpolate.griddata is used. For 2D data the griddata method supports three different methods “nearest”, “linear”, and “cubic”. For the nearest method a k-d tree is built using the scipy.spatial.cKDTree method in order to find the nearest neighbour. The linear method constructs a triangulation of the input data using the Qhull-library [32] and then performing barycentric interpolation on each triangle. In contrast, the cubic interpolation method performs a piecewise cubic interpolating Bezier polynomial on each triangle after the triangulation, see also [33]. These images have been taken with the inner (highest) frequency of 1 MHz and a outer (lowest) frequency of ~1 kHz. The used waveform generator allows an output frequency of up to 15 MHz. Each data point is represented by four float values (X,Y,X,V).With this setup we can easily achieve a frame rate up to 45 frames/s with a data rate of about 41 Mbit/s. Since this is not yet fast enough to follow the transitions from the crystalline to the vitreous phase in real space, we do not start with the recording in the center of the spiral but a little further outside (about 10% of the radius). This allows us to speed up the scanning by a factor of 100. With this modification we could scan with about 4500 frames/s and would end up with a data rate of about 4.1 Gbit/s.

RTEMS 4.12 - a real-time operating system is necessary to use the system within the intended scope. As operating system RTEMS was selected since we were no longer willing to pay the license costs for VxWorks. The new EPICS pvAccess protocol is used to meet the high data transfer requirements [34]. This efficient protocol makes intensive use of the shared pointers from the C++ TR1 Library Extension. Therefore, with the help of Sebastian Huber (embedded brains) [35] RTEMS 4.12 was successfully ported to the MVME6100 (beatnik) and to the MVME2500 board. Both ports are public available through den RTEMS source builder system [36]. EPICS (epics-base and epicsv4 modules) has been expanded to fully support RTEMS 4.12 and is fully supported from EPICS7 onwards. The RTEMS C Expression Shell is not yet implemented. This is to be done next. In the system, two single board systems are initially provided. The MVME6100 is responsible for the control of the hardware (waveform generator, digitizer), while the MVME2500 is dedicated to the communication with other

ISBN: 978-3-95450-193-9 doi:10.18429/JACoW-ICALEPCS2017-THPHA154

systems like storage, archiver and user interface. Communication between the two CPUs takes place via the VMEbus (up to 320 Mbyte/s). In the first version, we use 2 Gbit/s network interface on the VME2500 to transfer the obtained images. As the RTEMS 4.12 supports Symmetric Multiprocessing (SMP) both interfaces can run in parallel at full speed. With current hardware combination we can transfer up to about 1000 frames/s. If necessary, the system can be expanded with additional MVME2500 boards to increase the frame rate.

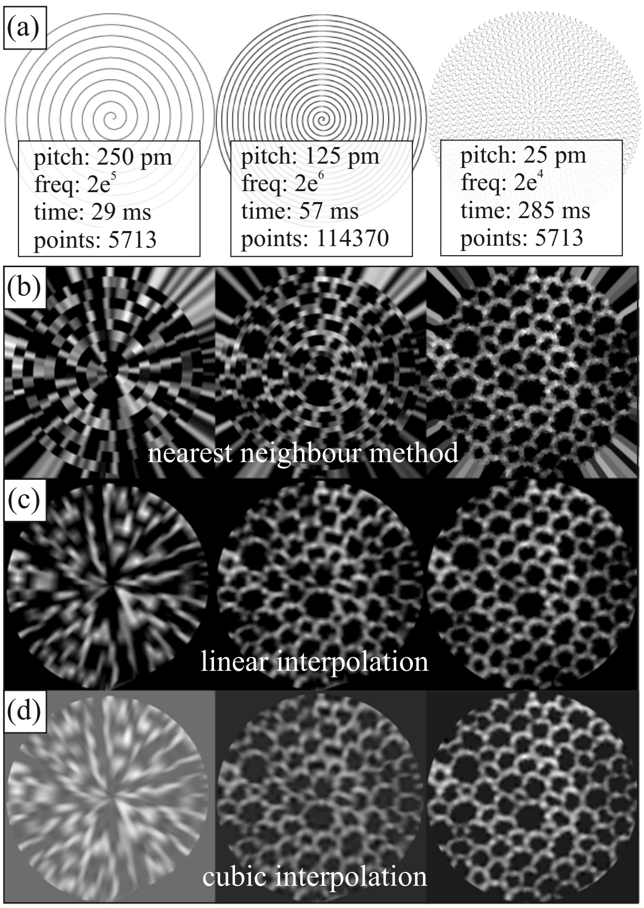

Figure 6: Spiral scans and interpolation results

A python-based software is developed to monitor the data stream (pvAccess) from the VMEbus system to the archiver and to present the operator almost every second a live image. The implementation p4p of Michael Davidsaver is used as a basis [37]. This makes it possible to intervene and to follow the measurement. In order to give the experimenters the opportunity to use Low energy electron diffraction (LEED), the system will also be equipped with a CCD camera AVT Mako-125 [38]. To read out and control this GigE camera the EPICS areadetector framework is used. The aravis lib is used and the camera interface follows the GenICam standard.

INSTITUTE ENVIRONMENT

The previously used EPICS ChannelArchiver was replaced by the ArchiverAppliance developed by Murali Shankar at SLAC to support archiving of structured PVs by the pvAccess protocol [39]. We run two server systems in a cluster configuration. These systems are equipped with 128 GByte main memory, 4 SSDs and two 10 Gbit/s ethernet interfaces. The ArchiverAppliance can use multiple stages of storage. For the short term storage (STS) we use 64 GByte of the main memory (ramdisk) with the granularity of an hour. The mid term storage (MTS) with the granularity of one day is realized with SSD storage. These two storage areas are local to the server systems. For the long term storage (LTS) both systems are using our central storage pool (NetApp) with the granularity "forever". The connection to the storage pool is realized with four 10 Gbit/s ethernets, NFS is used to mount the LTS. The data obtained from the experiments are monitored by the archiverAppliance and if changes happen the data set will be archived.

Every user who is involved in the project should have the possibility to monitor the state of the experiment independently of the computer system and operating system used. To control the CRYVISIL [40] experiment an IP-network was implemented. This CRYVISIL-LAN is isolated from the standard FHI-LAN by a gateway system. Through the use of EPICS based on the channel-access protocol (CA) and pvAccess (PVA) for communication all machine states (represented by so-called Process Variables (PVs)) can be monitored and controlled within the CRYVISIL-LAN by every connected system. The access from the FHI-LAN to the PVs is realized by a Channel- Access- and a pva2pva-proxy running on the gateway system. The PVs can be accessed from almost any software (Control System Studio (CSS), Matlab, LabVIEW, Python, Perl, C, C++, Web-Browser,...)

The operator interface is based on CSS [41]. As most of these applications deal with process variables and connections to control systems, the CSS Core provides the necessary APIs for dealing with them. Taking advantage of modern graphical editor software technology, Operator Interface (OPI) editor and runtime - Best OPI, Yet (BOY) - have been developed by the CSS collaboration. The Operator Interface is one of the basic components of the standard control system model. It provides scientists and engineers a rich graphical interfaces to view or operate the microscope locally or remotely.

ACKNOWLEDGEMENT

This project has received funding from the European Research Council (ERC) under the European Union's Horizon 2020 research and innovation programme (grant agreement no 669179). The authors acknowledge the great support from the insitute work shops.

REFERENCES

[1] EPICS, `https://github.com/epics-base`.

[2] Adrian C. Wright. Neutron scattering from vitreous silica. v. the structure of vitreous silica: What have we learned from 60 years of diffraction studies? *Proceedings of the First PAC RIM*

ISBN: 978-3-95450-193-9 doi:10.18429/JACoW-ICALEPCS2017-THPHA154

Meeting on Glass and Optical Materials, 179(Supplement C):84–115, November 1994.

[3] Leonid Lichtenstein, Christin Büchner, Bing Yang, et al. The atomic structure of a metal-supported vitreous thin silica film. *Angewandte Chemie International Edition*, 51(2):404–407, 2012.

[4] William Houlder Zachariasen. The atomic arrangement in glass. *Journal of the American Chemical Society*, 54(10):3841–3851, 1932.

[5] Leonid Lichtenstein, Markus Heyde, and Hans-Joachim Freund. Crystalline-vitreous interface in two dimensional silica. *Physical Review Letters*, 109(10):106101, 2012.

[6] Pinshane Y Huang, Simon Kurasch, Jonathan S Alden, et al. Imaging atomic rearrangements in two-dimensional silica glass: Watching silica's dance. *science*, 342(6155):224–227, 2013.

[7] Hans-Joachim Freund. Controlling silica in its crystalline and amorphous states: A problem in surface science. *Accounts of Chemical Research*, 50(3):446–449, 2017.

[8] Ahmed H. Zewail. Femtochemistry: Atomic-scale dynamics of the chemical bond using ultrafast lasers (nobel lecture). *Angewandte Chemie International Edition*, 39(15):2586–2631, 2000.

[9] Sebastian Loth, Markus Etzkorn, Christopher P. Lutz, D. M. Eigler, and Andreas J. Heinrich. Measurement of fast electron spin relaxation times with atomic resolution. *Science*, 329(5999):1628–1630, 2010.

[10] Yasuhiko Terada, Shoji Yoshida, Osamu Takeuchi, and Hidemi Shigekawa. Real-space imaging of transient carrier dynamics by nanoscale pump-probe microscopy. 4:869, October 2010.

[11] Tyler L. Cocker, Vedran Jelic, Manisha Gupta, et al. An ultrafast terahertz scanning tunnelling microscope. 7:620, July 2013.

[12] Tyler L. Cocker, Dominik Peller, Ping Yu, Jascha Repp, and Rupert Huber. Tracking the ultrafast motion of a single molecule by femtosecond orbital imaging. *Nature*, 539(7628):263–267, November 2016.

[13] J. Wintterlin, J. Trost, S. Renisch, et al. Real-time stm observations of atomic equilibrium fluctuations in an adsorbate system: O/ru(0001). *Surface Science*, 394(1):159–169, December 1997.

[14] Lindsay R. Merte, Guowen Peng, Ralf Bechstein, et al. Water-mediated proton hopping on an iron oxide surface. *Science*, 336(6083):889–893, 2012.

[15] G. Aad, B. Abbott, J. Abdallah, et al. Charged-particle multiplicities in pp interactions measured with the atlas detector at the lhc. *New Journal of Physics*, 13(5):053033, 2011.

[16] Guocai Dong, Elodie B. Fourré, Femke C. Tabak, and Joost W. M. Frenken. How boron nitride forms a regular nanomesh on rh(111). *Phys. Rev. Lett.*, 104:096102, Mar 2010.

[17] C. Sachs, M. Hildebrand, S. Völkening, J. Wintterlin, and G. Ertl. Reaction fronts in the oxidation of hydrogen on pt(111): Scanning tunneling microscopy experiments and reaction-diffusion modeling. *The Journal of Chemical Physics*, 116(13):5759–5773, April 2002.

[18] J. Wintterlin, S. Völkening, T. V. W. Janssens, T. Zambelli, and G. Ertl. Atomic and macroscopic reaction rates of a surface-catalyzed reaction. *Science*, 278(5345):1931, December 1997.

[19] M. J. Rost, L. Crama, P. Schakel, et al. Scanning probe microscopes go video rate and beyond. *Review of Scientific Instruments*, 76(5):053710, May 2005.

[20] M. J. Rost, G. J. C. van Baarle, A. J. Katan, et al. Video-rate scanning probe control challenges: setting the stage for a microscopy revolution. *Asian Journal of Control*, 11(2):110–129, 2009.

[21] SPECS nanonis SPM, `http://www.specs-zurich.com/en/SPM-Control-System.html`.

[22] FEMTO, `http://www.femto.de/en`.

[23] MOXA, `https://www.moxa.com`.

[24] ASYN, `https://github.com/epics-modules/asyn`.

[25] StreamDevice, `http://epics.web.psi.ch/software/streamdevice/`.

[26] CA Lab, `https://www.helmholtz-berlin.de/zentrum/locations/it/software/exsteuer/calab/index_en.html`.

[27] LabVIEW, `http://www.ni.com/en-us/shop.html`.

[28] Markus Heyde, Georg H Simon, and Leonid Lichtenstein. Resolving oxide surfaces–from point and line defects to complex network structures. *physica status solidi (b)*, 250(5):895–921, 2013.

[29] V375, `http://www.highlandtechnology.com/DSS/V375DS.shtml`.

[30] I. A. Mahmood, S. O. R. Moheimani, and B. Bhikkaji. A new scanning method for fast atomic force microscopy. *IEEE Transactions on Nanotechnology*, 10(2):203–216, March 2011.

[31] SIS3316, `http://www.struck.de/sis3316.html`.

[32] Qhull-library, `http://www.qhull.org`.

[33] Eric Jones, Travis Oliphant, Pearu Peterson, et al. SciPy: Open source scientific tools for Python, 2001–.

[34] pvAccess, `http://epics-pvdata.sourceforge.net/pvAccess_Protocol_Specification.html`.

[35] embedded brains, `http://www.embedded-brains.de`.

[36] RTEMS source builder, `https://docs.rtems.org/branches/master/rsb/source-builder.html`.

[37] p4p, `https://github.com/mdavidsaver/p4p`.

[38] AVT Mako-125, `https://www.alliedvision.com/en/products/cameras/detail/Mako%20G/G-125.html`.

[39] archiverAppliance, `https://slacmshankar.github.io/epicsarchiver_docs/`.

[40] G:(EU-Grant)669179, CRYVISIL, `http://cordis.europa.eu/project/rcn/198020_en.html`.

[41] Control System Studio, `https://github.com/ControlSystemStudio`.